J Solid State Electrochem (1999) 3: 245–250 © Springer-Verlag 1999

ORIGINAL PAPER

W.R. Fahrner · G. Grabosch · D. Borchert
Y. Chan · S. Kwong · K. Man

Temperature dependency of the intrinsic carrier density of hydrogenated amorphous silicon in MOS structures

Received: 17 June 1998 / Accepted: 23 October 1998

Abstract The admittance versus frequency of a hydrogenated amorphous silicon metal oxide semiconductor capacitor is measured at a fixed bias in inversion and for temperatures in the range of 20–50 °C. The data are fitted to theoretical capacitance and conductance curves where the time constant of inversion is the result of the fit. In turn, the time constant can be converted to the (minority) carrier lifetime so that a lifetime value for each measurement temperature is available. The conversion from the time constant to the minority carrier lifetime requires the knowledge of the temperature-dependent intrinsic carrier density or rather its activation energy. The criterion for the correct choice is a temperature-independent carrier lifetime. Three published room temperature values of the intrinsic carrier density have been tested. The carrier lifetime activation energy is $E_a = 0.70 \pm 0.03$ eV.

Key words Hydrogenated amorphous silicon · Metal oxide semiconductor · Intrinsic carrier density · MOS dispersion measurement

Introduction

Published data on the intrinsic carrier density

Many material parameters known for decades for monocrystalline silicon are still controversially discussed in the case of hydrogenated amorphous silicon (a-Si:H). A typical example is the intrinsic carrier density, n_i. A first a-Si:H room temperature value had been derived when introducing the equivalent state densities $N_c = N_v = 2 \times 10^{20}$ cm^{-3} [1, 2] and activation energies of $E_a = 0.65$ eV [1] and 0.77 eV [2] into the usual Fermi statistics expression $n_i = \sqrt{(N_c N_v)} \exp(-E_a/k\theta)$, where θ is the temperature. The discrepancy in the activation energy was removed later by an improved value $E_a = 0.86$ eV and densities $N_c = N_v = 1 \times 10^{20}$ cm^{-3} [3] so that $n_i = 2.(58) \times 10^{-5}$ cm^{-3} was deduced. Other authors report $n_i = 1 \times 10^7$ cm^{-3} [4], and 4.3×10^8 cm^{-3} [5], so that a span of more than three orders of magnitude is observed. This fact justifies a closer examination of the intrinsic carrier density.

The metal oxide semiconductor structure as used for measuring semiconductor properties

As an appropriate tool we have chosen a metal oxide semiconductor (MOS) structure with a-Si as the semiconductor. We measure the capacitance and the conductance as a function of frequency while the applied inversion bias is kept constant. Typical results of such a dispersion measurement are a step-like curve for the capacitance C and a bell-shaped curve for the (frequency normalized) conductance G/f. (f being the frequency). It has been shown [6–8] that the frequency f^* for which the step of C or the bell maximum of G/f occur bears information on the lifetime, τ, of the semiconductor. The relaxation time as the time constant of inversion

$$T = 1/2\pi f^* \tag{1}$$

is related to the carrier lifetime τ by:

$$T/\tau = N_D/n_i \tag{2}$$

where N_D is the (donor) doping level. Equation 2 is the well-known Zerbst relaxation time constant originally deduced for the large pulse biases. It is also valid for the above small signal case.

When the temperature θ is increased, n_i will follow a law derived from Fermi statistics here written in the

W.R. Fahrner (✉) · G. Grabosch · D. Borchert
Chair of Electronic Devices, P.O. Box 940,
University of Hagen, D-58084 Hagen, Germany

Y. Chan · S. Kwong · K. Man
City University of Hong Kong,
Kowloon, Hong Kong

form:

$$n_i = n_{i0} \exp(-E_a/k\theta) \tag{3}$$

(For monocrystalline silicon n_{i0} is identified with $\sqrt{N_c N_v}$, where N_c and N_v are the conduction and valence band state densities, and E_a with half of the bandgap energy). Since N_D and – to a first order approximation – τ are independent of θ, the temperature dependence of T is an inverse measure of that of n_i.

MOS evaluation for defect-rich substrates

Equation 2, however, is true only in the case of monocrystalline silicon or, rather, for a material with a defect concentration low compared to the doping level. Below we will briefly repeat the generalization of Eq. 2 for defect-rich materials such as a-Si:H. A second generalization is required for the calculation of the $C(2\pi fT)$ and $G(2\pi fT)/(2\pi fT)$ *versus*. $2\pi fT$ curves. It turns out that the measured curves are broader than predicted by simple Debye theory.

Experimental

A specially designed MOS structure (Fig. 1) has been used. It consists of an *n*-type monocrystalline silicon wafer of high doping concentration. The wafer is thermally oxidized and covered with nominally undoped a-Si:H (in fact the a-Si is of n^--type with a doping level of $N_D = 7 \times 10^9$ cm^{-3}). Phosphorus is added to the silane at the end of the deposition process to provide a good ohmic contact to the metal evaporated on top of the n^{2+}-a-Si:H. A mesa Al/a-Si:H structure is obtained after photolithography and dry etching. For details of the process parameters we refer to [8, 9], which also include a collection of the resulting electrical data.

The capacitance, C, and conductance, G, versus frequency, f, at a fixed inversion bias have been measured on this device. An example for these measurements is given in Fig. 2a and b. The step in C and the bell in $G/2\pi f$ are clearly visible (for technical reasons the low frequency portions of the curves are not complete, an effect which is caused by the inaccuracy of the bridge in this regime). The transition frequency moves towards higher values with increasing temperature, as expected from Eq. 2.

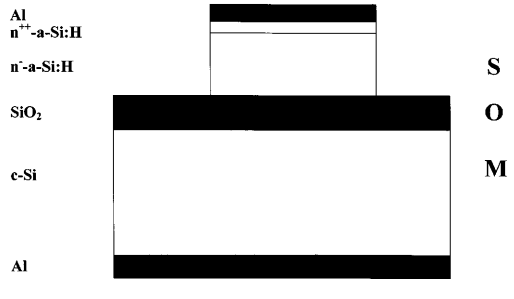

Fig. 1 Cross section of the a-Si MOS structure. $N_{D+} = 10^{19}$ cm^{-3}, $N_{D-} = 7 \times 10^9$ cm^{-3}, $d_{a\text{-}Si} = 0.65$ µm, $\rho_{c\text{-}Si} < 0.015$ Ω cm. The manufacturing process is given in [9]

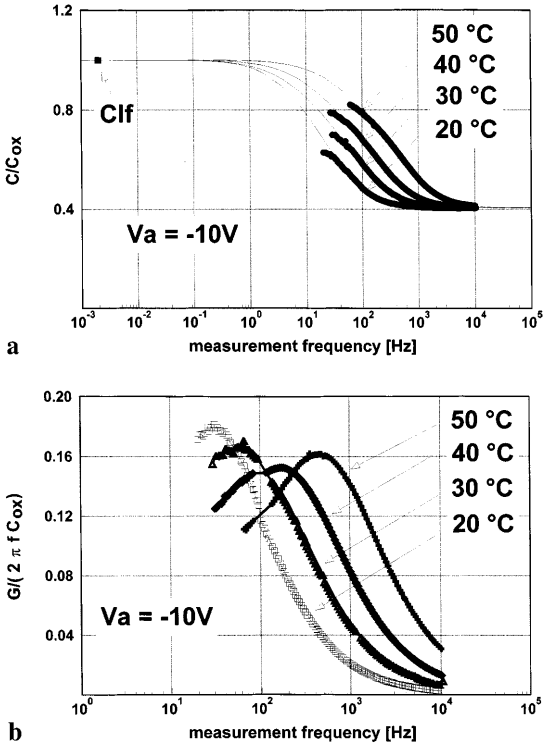

Fig. 2 a Measured (*circles*, *square*) and calculated (Eq. 8; *hairline*) dispersion for C; C_{lf} is the result of a slow ramp capacitance measurement. **b** Measured dispersion for $G/2\pi f$

Theory

Debye relaxation of the a-Si MOS admittance in inversion

In a first approach the relaxation time constant T can be extracted from these measurements according to [6, 7] by means of:

$$\frac{C}{C_{ox}} = \frac{1 + (C_{min}/C_{ox})(\omega T)^2}{1 + (\omega T)^2} \tag{4}$$

$$\frac{G}{\omega C_{ox}} = \frac{\omega T(1 - C_{min}/C_{ox})}{1 + (\omega T)^2} \tag{5}$$

where $\omega = 2\pi f$, C_{ox} is the oxide capacitance, and C_{min} the minimum capacitance in a high frequency C-V measurement. In [8] it has been shown that the scaling factor N_D/n_i between T and τ, Eq. 2, must be generalized for the case of trap-rich material:

$$\frac{T}{\tau} = \frac{(Q_{sc\approx} + u_{s\approx} C_{ax})/q}{Bn_i} \tag{6}$$

$Q_{sc\approx}$ is the space charge increment (total charge, Q_T, minus inversion charge, Q_I) in the a-Si layer, when the

inversion surface potential is increased by $u_{sc\approx}$. Bn_i is the charge increment of the minority carriers, where B is a factor correcting for the lifetime ratio τ_n/τ_p and the finite a-Si layer width. An important contribution to $Q_{sc\approx}$ is the trap charge in the bulk states. Their distribution is assumed to be $N_b = N_{b0} \cosh(\psi_s/\psi_c)$ in agreement with [4, 8] (ψ_s is the surface potential in volts, ψ_c a slope parameter, $\psi_c = 0.1$ eV in this work, [10]). Let us add for the following considerations that the calculation of T/τ requires the knowledge of n_i and its temperature dependency.

Equation 6 is the result of a charge redistribution analysis for two neighboring surface potentials and Shockley-Read-Hall statistics [6, 8]. Thus, if the right-hand side scaling factor of Eq. 6 is known from numerical calculations [8] and T is known from fitting Eq. 4 or 5 to the measured data, one could obtain the lifetime τ. We have observed, however, that in many cases the measured dispersion curves are broader than expected from the above theory. Figure. 3a and b deliver a comparison of measured data with the predictions of Eqs. 4 and 5. Thus we now introduce statistical fluctuations as a broadening mechanism and apply the resulting dispersion to the measured data.

The dispersion model

In the following we take up an earlier concept of Nicollian and Götzberger [11]. They measured the conductance caused by MOS surface states and found a much broader dispersion than expected. Their generally accepted explanation was a statistically distributed surface potential, which is also assumed in our case. Such a distribution might have several physical origins: locally varying oxide charges, oxide thicknesses, doping levels, bulk and surface state densities, etc. We will summarize all these effects in a common statistical description. Now we assume the total MOS dot area to be subdivided into sufficiently small subareas, each of them being small enough to ensure a constant surface potential within this subarea. It might be assumed that the resulting u' is Poisson distributed around the mean value u_s induced by the applied voltage and – owing to the large number of subareas and the large number of charges residing per subarea – that the Poisson distribution specializes into the Gaussian distribution described by a standard deviation σ:

$$p(u') = \frac{1}{\sigma\sqrt{2\pi}} \exp[-(u' - u_s)^2/2\sigma^2]$$

so that

$$\frac{C}{C_{ox}} = \frac{1}{\sigma\sqrt{2\pi}} \int_{-\infty}^{\infty} \frac{1 + (\omega\tau\, T(u')/\tau)^2 (C_{min}/C_{ox})}{1 + (\omega\tau T(u')/\tau)^2} \times \exp[-(u' - u_s)^2/2\sigma] du' \tag{8}$$

and

$$\frac{C}{\omega C_{ox}} = \frac{1}{\sigma\sqrt{2\pi}} \int_{-\infty}^{\infty} \frac{1 + (\omega\tau\, T(u')/\tau)(1 - C_{min}/C_{ox})}{1 + (\omega\tau T(u')/\tau)^2} \times \exp[-(u' - u_s)^2/2\sigma] du' \tag{9}$$

In the derivation of Eqs. 8 and 9 it has been tacitly assumed that T is a function of u' (otherwise no curve broadening would be seen). This assumption has been checked by a numerical calculation of the right side of Eq. 3. For each temperature the finite element method (FEM) of [8] is applied for a series of surface potentials so that a data set for T/τ versus u' is generated. $N_{b0} = 9 \times 10^{16}$ V^{-1}cm^{-3} and $\psi_c = 0.1$ V, required for the calculations were known from [10].

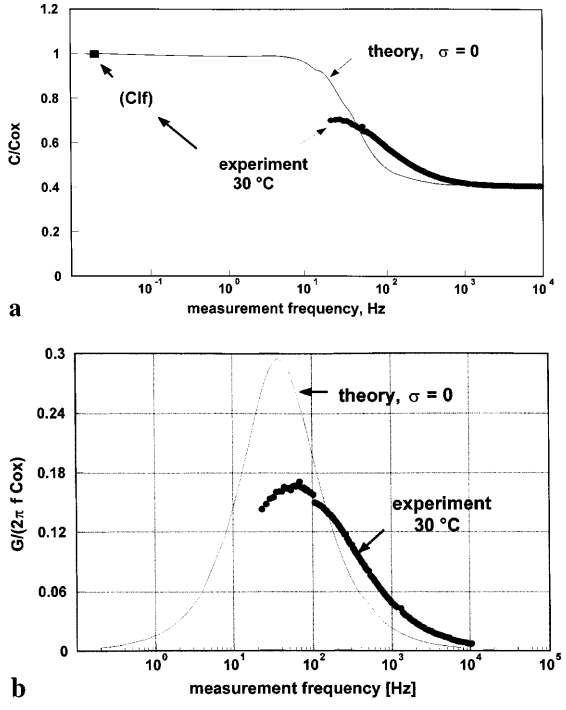

Fig. 3 **a** Experimental $C(f)$ curve (*circles*) and theoretical $C(f)$ curve according to Eq. 4. **b** Experimental $G(f)/2\pi f$ curve (*circles*) and theoretical $G(f)/2\pi f$ curve according to Eq. 5

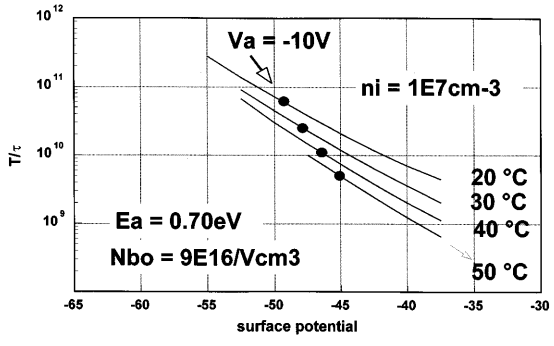

Fig. 4 T/τ versus u_s for the sample of Fig. 1. Temperatures are 20, 30, 40, and 50 °C, the trap density $N_{b0} = 9 \times 10^{16}$ V^{-1}cm^{-3}, and the activation energy $E_a = 0.70$ eV

A typical result is seen in Fig. 4. The shape of these curves strongly depends on the assumed values of n_i and even more on the bulk state densities. T/τ versus u' is inserted in Eqs. 8 and 9. C and G should be calculated for a frequency range which contains the transition from low frequency behavior to high frequency behavior of the MOS capacitance. For the numerical calculation it is thus preferable to avoid ω as the frequency variable for $C(\omega)$ and $G(\omega)/\omega$ but rather to transform $(\omega\tau T(u')/\tau)$ of Eqs. 8 and 9 to the expression

$$\omega T(u_s)\frac{T(u')/\tau}{T(u_s)/\tau}$$

where u_s stands for the surface potential induced by the measurement bias, V_a. The right side fraction roughly varies between 0.01 and 100. Thus if $\omega T(u_s)$ is chosen as the "frequency" variable, it will always show full dispersion of C and G/ω in the range of, say, 0.001 and 1000.

u_s is given by the choice of the applied voltage. For a given surface potential the numerical solution of Poisson's equation [8] delivers the surface field of the semiconductor. From the continuity of the displacement density D we can calculate the oxide voltage V_{ox} and subsequently the externally applied voltage V_a. The search for the correct u_s (yielding $V_a = -10$ V) is done with an interpolation routine. There is virtually no contribution of fixed oxide charges to the total voltage. This has been demonstrated [10]. In addition, we do not expect any dependency of the dispersion on the inversion bias if the latter is large enough.

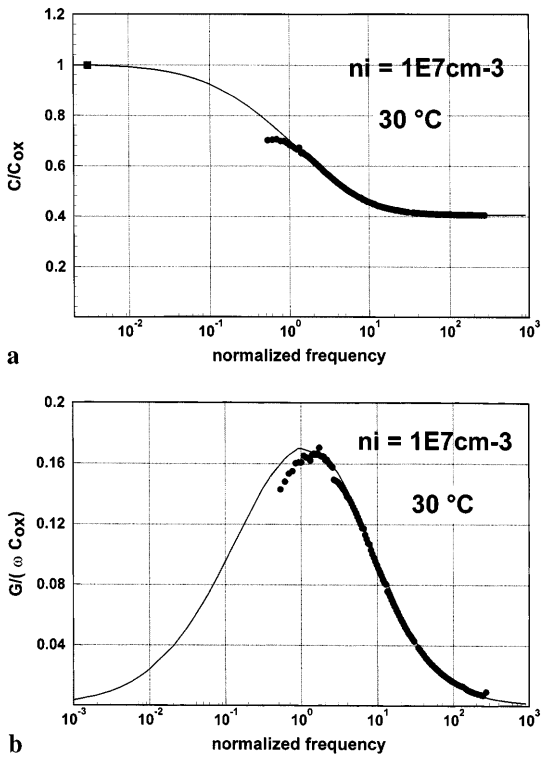

Fig. 5 **a** Theoretical (*full line*) and measured capacitance (*circles*, *square*); $\theta = 30$ °C, standard deviation $\sigma = 6$. **b** Theoretical (*full line*) and measured frequency normalized conductance (*circles*); $\theta = 30$ °C, standard deviation $\sigma = 6$

Results

In Fig. 5a and b we have redrawn the 30 °C capacitance and frequency normalized conductance measurements of Fig. 2a and b. In the same figure we have inserted the result of a fit according to Eqs. 8 and 9. The surface potential was −47.89 for $V_a = -10$ V; $T(u')/\tau$ was taken from Fig. 4. Guess values $n_{i0} = 8.(37)\ \text{cm}^{-3}$ and $E_a = 0.70$ eV have been used resulting in $n_i = 1.88 \times 10^7\ \text{cm}^{-3}$. The standard deviation turned out to be $\sigma = 6$.

It should be pointed out that several sharp criteria for the validity of the fit are given:

1. The same σ must describe both admittance components, capacitance and conductance.
2. The same time constant must be found for the two components. For the fitting procedure this means that the same vertical shift Δf (along the frequency) axis must apply when looking for coincidence of the calculated capacitances and conductances with the measured ones.
3. In contrast to the conductance method for surface state density determination, there is no vertical shift allowed which would shift the theoretical into the measured $G/\omega C_{ox}$ curves. This means that especially the $G/\omega C_{ox}$ maxima from theory and experiment must coincide (the last criterion permits a reliable determination of σ and f^*). Except for low frequencies, where the measurement bridge becomes inaccurate, the coincidences are good.

From this fit we have all the necessary information to deduce the lifetime which is $\tau = 1.67 \times 10^{-13}$ s.

With the same guess values $n_{i0} = 8.(37)\ \text{cm}^{-3}$ and $E_a = 0.70$ eV the above procedure has been repeated for the other temperatures (20, 40, and 50 °C) so that a complete set of $\tau(\theta)$ is available.

Of course, we expect a temperature-independent τ. The way to reach this goal is the correct choice of the guess values in the fit. According to Eq. 3 two unknown parameters, n_{i0} and E_a, are required to cover the full temperature range. On the other hand, two pieces of information are available: the room temperature (say 23 °C) n_i of one of [3–5] and the independence of τ on θ at least in the temperature range 20–50 °C. Thus for a set of E_a, 0.9 eV ≥ 3 $E_a \geq 3$ 0.6 eV, we have calculated the resulting n_{i0} values based on the n_i(23 °C) value from one of the [3–5]. This also yields the n_i values for 20, 30, 40, and 50 °C. Subsequently the τ values have been deduced after fitting for each temperature. A typical result is one of the curves of Fig. 6, where the obtained τ versus $1000/k\theta$ have been plotted. In this case, $E_a = 0.70$ eV

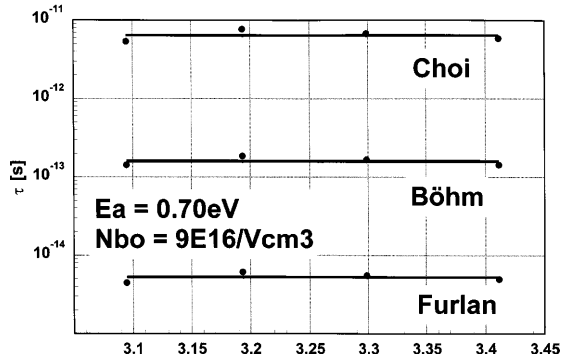

Fig. 6 Lifetime τ versus inverse temperature $1000/k\theta$

had been chosen. The standard deviation $\Delta\tau$ of the data points from the horizontal average has been recorded. After repeating this procedure for the entire E_a set, a curve of $\Delta\tau/\tau$ versus E_a is generated for each of the 23 °C n_i values (Fig. 7). These curves exhibit a minimum at 0.70 eV. For higher or lower E_a the τ versus $1000/k\theta$ curves show negative or positive slopes. Thus we conclude that an activation energy of $E_a = 0.70 \pm 0.03$ eV is valid. The resulting data are compiled in Table 1.

Finally, we present the dependency of n_i on (inverse) temperature for the three starting n_i values (Fig. 8). The above activation energy of 0.70 eV has been assumed.

Discussion

In the case of a monocrystalline semiconductor, theory predicts that the activation energy of n_i is identical to half of the bandgap energy while n_i itself is given by

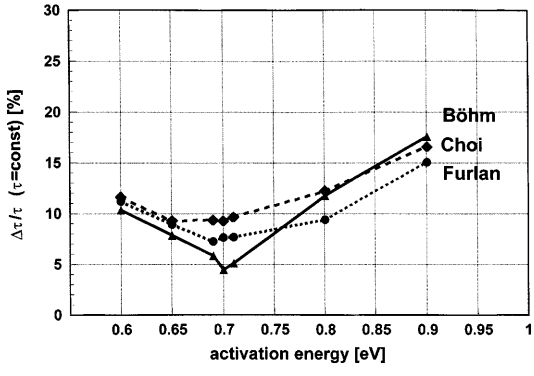

Fig. 7 Normalized standard deviation $\Delta\tau/\tau$ versus activation energy E_a

$\sqrt{N_c N_v}\exp(-E_a/k\theta)$. Though it is questionable whether this concept can be transferred in full to amorphous silicon, it is worthwhile comparing our data with the commonly accepted parameters of a-Si. Our activation energy (0.70 eV) is smaller than half of the (optically measured) bandgap, E_G. From a Tauc plot we have deduced $E_G = 1.8$ eV or slightly below. Most of the discrepancy is explained by the potential fluctuations. A comprehensive survey on their effects has been given by Overhof and Thomas [12]. They derive an expression for doped amorphous material, which gives a potential fluctuation of 0.2 eV (a trap density of 10^{16} V^{-1} cm^{-3} is assumed). They also point out that there exist other sources of potential fluctuations. No definite figure is given for these effects. from our measurements, however, we are able to extract the value of the potential fluctuation: from the fit of Fig. 5, a potential fluctuation ($=\sigma$) of 6 was found which is equivalent to $\sigma\, k\theta/q \approx 0.16$ eV for 30 °C. This figure is almost identical to the above theoretical value of Overhof and Thomas. For any location in the amorphous layer and any energy position, E^*, between the valence and conduction band, the energy distance between E^* and the valence band, E_V, will vary between $(E^* - E_V) \pm 0.16$ eV. The analog relation holds for the conduction band. Thus there will be combinations for which E^* sees an effective band gap of $E_G - (2 \times 0.16)$ eV. We assume that for generation recombination the carriers are supplied from the lowest edge of the conduction band and the highest edge of the valence band. Half of the above value, i.e. 0.74 eV, is already very close to our measured activation energy, 0.70 eV.

On the base of the above measurements solely, no unambiguous decision can be made in favor of one of the starting n_i values. However, we tend to exclude the n_i of [3] as a starting parameter for three reasons:

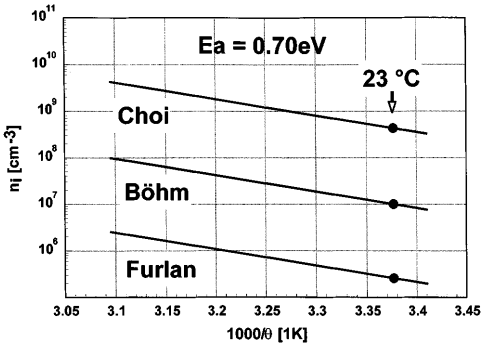

Fig. 8 Intrinsic carrier n_i density *versus.* inverse temperature $1000/k\theta$

Table 1 Comparison of experimental and literature data

Ref.	n_i [cm^{-3}] (23 °C)(ref)	E_a (eV) (ref)	E_a (eV) (exp)	N_c, N_v (cm^{-3}) (ref)	n_{i0} (cm^{-3}) (exp)	τ(s) (exp)
3	2.58×10^5	0.86	0.70	1×10^{20}	2.16×10^{17}	5.24×10^{-15}
4	1×10^7		0.70		1.24×10^{19}	1.59×10^{-13}
5	4.3×10^8		0.70		3.60×10^{20}	6.41×10^{-12}

1. A lifetime value of 5×10^{-15} s is extremely small even for the heavily disturbed a-Si structure. The data of diffusion length and mobility in [13] hint at a minimum lifetime in the picosecond range.
2. The same is true if the concept of $n_{i0} = \sqrt{N_c N_v}$ is adopted. A value $\sqrt{N_c N_v} = 2.2 \times 10^{17}$ cm^{-3} appears to be very low.
3. The calculated C_{lf} curve (not shown) based on $n_i = 2.58 \times 10^5$ cm^{-3} would require a *negative* oxide charge density of $Q_{ox} = 3.4 \times 10^{11}$ cm^{-2} to be fitted to the experimental curve. However, negative charges have never been observed in a thermal oxide.

Comparing the results based on the starting values of [4] and [5] we slightly favor the room temperature n_i of [4]: it has been the result of a fit to experimental thin film transistor (TFT) data. The 10^7 cm^{-3} value is especially able to explain the measured off conductance of a TFT. This condition is much more stringent than the weaker test for agreement of theoretical and measured *C-cV* curves solely used in [5].

Conclusion

Admittance measurements of an a-Si:H MOS diode as function of frequency and temperature have been performed. The results are presented in terms of three different published values of intrinsic carrier concentration n_i. All three values indicate an activation energy of 0.70 eV. The smallest n_i value of 2×10^5 cm^{-3} can be probably ruled out.

Acknowledgements This work has been made possible by the financial help of the AG Solar, North-Rhine Westphalia. We are grateful to our colleagues Dr. Löffler and Dr. Neitzert for communicating their data prior to publication.

References

1. Topic M, Smole F, Furlan J, Fortunato E, Martins R (1996) Mater Res Soc Symp Proc 420: 171
2. Smole F, Groznik A, Topic M, Popovic P, Furlan J (1996) Mater Res Soc Symp Proc 420: 221
3. Furlan J (1997) Personal communication
4. Böhm M, Houghton J, Salamon S (1987) The influence of bulk and interface gap states on the performance of amorphous silicon transistors. Mater Res Soc spring meeting, Anaheim, Calif., p 481
5. Choi JS, Neudeck GW (1992) IEEE Trans Electron Devices 39: 2515
6. Nicollian EH, Brews JR. (1982) MOS (metal-oxide-semiconductor) physics and technology. Wiley, New York, pp 134–141
7. Klausmann E, Fahrner WR, Löffler S, Neitzert HC (1993) J Electrochem Soc 140: 2323
8. Fahrner WR, Löffler S, Klausmann E, Neitzert HC (1994) J Electrochem Soc 141: 2151
9. Neitzert HC, Löffler S, Klausmann E, Fahrner WR (1994) J Electrochem Soc 141: 2151
10. Fahrner WR, Löffler S, Chan Y, Kwong S, Man K (1998) J Electrochem Soc 145: 1786
11. Nicollian EH, Goetzberger A (1967) Bell Syst Tech J 46: 1055
12. Overhof H, Thomas P (1989) Hydrogenated amorphous semiconductors. Springer Berlin, Heidelberg New York p 108
13. The Institute of Electrical Engineers (ed) (1989) Properties of amorphous silicon, 2nd edn. Inspec, London